J. Meas. Sci. Instrum., 2025, 16(2): 236-244. http://jmsi.publish.founderss.cn
DOI: 10.62756/jmsi.1674-8042.2025023 jmsi@nuc.edu.cn

Multi-information fusion algorithm for temperature prediction based on MP-Huber Kalman filter

XU Wanjin, LI Jiying*, LU Yandong

School of Electronic and Information Engineering, Lanzhou Jiaotong University, Lanzhou 730070, China

***Corresponding author:** LI Jiying (ljy7609@126.com)

Received: August 20, 2023 **Revised:** October 11, 2023 **Accepted:** November 18, 2023

Abstract: In order to reduce the error judgment of outliers in vehicle temperature prediction and improve the accuracy of single-station processor prediction data, a Kalman filter multi-information fusion algorithm based on optimized P-Huber weight function was proposed. The algorithm took Kalman filter (KF) as the whole frame, and established the decision threshold based on the confidence level of Chi-square distribution. At the same time, the abnormal error judgment value was constructed by Mahalanobis distance function, and the three segments of Huber weight function were formed. It could improve the accuracy of the interval judgment of outliers, and give a reasonable weight, so as to improve the tracking accuracy of the algorithm. The data values of four important locations in the vehicle obtained after optimized filtering were processed by information fusion. According to theoretical analysis, compared with Kalman filtering algorithm, the proposed algorithm could accurately track the actual temperature in the case of abnormal error, and multi-station data fusion processing could improve the overall fault tolerance of the system. The results showed that the proposed algorithm effectively reduced the interference of abnormal errors on filtering, and the synthetic value of fusion processing was more stable and critical.

Key words: Huber weight function; Mahalanobis distance; Kalman filter; mulit-information fusion; temperature prediction

0 Introduction

As far as the traditional temperature measurement system is concerned, the temperature prediction system can estimate the temperature of various environments in a relatively timely and effective manner. In the face of inherent problems, such as electrical and electronic sensor factory settings, aging, and damaged products, the temperature prediction model can correct the measurement error of the device itself in time. At the same time, temperature switching in temperature prediction model is also of great value in practical applications. For too high temperature in summer, too low temperature in winter, or large temperature changes in a short time, temperature prediction can effectively prevent the occurrence of car body and biological hazards. People's comfort temperature range is wider than that is recommended by current national or international standards[1], and temperature prediction can more effectively set the comfort temperature environment of the car. Predicting the temperature in the car can also prevent problems such as waste of air-conditioning energy caused by unreasonable temperature settings.

In order to realize the optimization process of the vector computer method, Pang et al. [2] adopted the particle swarm optimization algorithm. Sun et al. [3] proposed an algorithm called time-delay pruning in the sense of least squares. They achieved room temperature prediction under the physical laws of heat transfer in different indoor heating systems.

The improved Kalman recursive algorithm[4-6] is adopted in this paper, which not only eliminates the previous cases of particles tending to homogenization (loss of diversity), but also requires less storage space, which can deal with relatively stable processes and is more conducive to dealing with non-stationary processes and multidimensional objects. It greatly expands the scope of application. Due to the thin external components, strong thermal conductivity of the car body, and small space, the car body temperature is easily affected by the external environment. Therefore, compared with simple temperature measurement, the accurate prediction of the interior temperature of the car is more important practical significance for human and vehicle safety, environmental comfort, energy saving

and environmental protection. In the actual temperature measurement, it will be affected by many factors such as sudden changes in the external weather, the presence or absence of sunlight, the strength of air flow, the degree of sealing of the compartment, etc. It will lead to the occurrence of abnormal temperature error interference (the generation of wild value), and greatly reduce the temperature prediction accuracy.

This paper introduces M estimation into Kalman algorithm, uses Mahalanobis distance as the discriminant of M estimation to obtain the improved Kalman filtering algorithm based on M estimation with P-Huber weight functions (MP-Huber KF). The simulation results showed that the algorithm had good target tracking performance when there are abnormal errors, and the tracking effect was more accurate and stable. The average absolute errors are respectively 0.172 and 0.342. Furthermore, the temperature estimates at key positions in the vehicle were further processed by fusion algorithm to obtain effective values with smoothing effect, thereby improving the anti-wildness ability and the robustness of tracking filtering.

1 System model and Kalman filtering algorithm

1.1 System model

The system takes the temperature inside the car as the research object, as shown in Fig.1. According to the daily temperature experience, the indoor temperature of the car is set to fluctuate regularly within a certain range to simulate the changes in the outside weather, sunlight, air flow, and the degree of compartment sealing in the car body, resulting in temperature fluctuations that interfere with the display status[7].

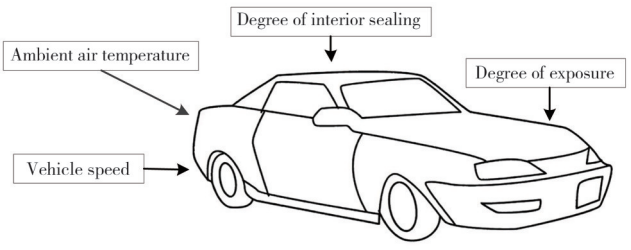

Fig. 1 Diagram of influencing factors of automobile indoor temperature

Assume that the external weather clouds vary greatly, causing sunlight to appear and disappear for a while, and the car is not in a sealed state, there is a small amount of air exchange. The unstable factor is the process noise in the model. W represents external weather changes, sunlight intensity, and air ventilation. Due to the electrical and electronic type of sensor out of the field settings, aging, damage products and other inherent problems, out of the field description indicates that the temperature sensor measurement error, so the data measured by the thermometer is not completely close to the real temperature, so that the measurement noise is V. State X is the number of minutes when room temperature data is available. The temperature data collected by the unit is used as the system input, and the temperature state observation equation in the vehicle is

$$X(k)=AX(k-1)+\Gamma W(k-1), \tag{1}$$

$$Z(k)=HX(k)+V(k), \tag{2}$$

where A is the state transfer equation; Γ is the state noise transfer equation; H is the state transfer relation and it is the relational value of the probability statistics of the system model. Since the system information is a one-dimensional array, then A and Γ are the numerical changes to $X(k)$. $Z(k)$ is the linear relational change of $X(k)$.

1.2 Kalman filter algorithm

The Kalman filter uses the linear system state equation to continuously input the original state and output the update observation data process[8-10]. Since the input/output relationship inherently represents the equation of state and the output equation, the estimated signal is regarded as the output of a random linear system under white noise. Therefore, the process is in a constant "prediction-correction" calculation among the various links[11-14]. As the highest real-time estimation algorithm, Kalman filter has a relatively wide range of applications in target positioning.

Step 1 KF predicts the state at moment k based on the state estimate at moment $k-1$. $j=k$, $j>k$, and $j<k$ represent the Kalman filter, forecaster, and smoother, respectively.

$$\hat{X}(k+1|k)=\Phi\hat{X}(k|k), \tag{3}$$

where $\hat{X}(k+1|k)$ is the linear variance estimate for state $X(j|k)$; Φ is the state transfer matrix.

Step 2 KF goes to the next status update. The Kalman filter gain is obtained according to the recursive projection theorem.

$$\hat{X}(k+1|k+1)=\hat{X}(k+1|k)+K(k+1)\varepsilon(k+1), \tag{4}$$

$$\varepsilon(k+1)=Y(k+1)-H\hat{X}(k+1|k), \tag{5}$$

$$K(k+1)=P(k+1|k)H^{\mathrm{T}}\left[HP(k+1|k)H^{\mathrm{T}}+R\right]^{-1}, \tag{6}$$

where $\varepsilon(k+1)$ is the new interest series, which is the difference between the existence value and the optimal forecast valuation; $K(k+1)$ is the Kalman filter gain; $\boldsymbol{H}$ is the relational value of the probability statistics of the system model; $\boldsymbol{P}(k+1)$ is defined quality advantages and disadvantages artificially.

Step 3 KF predicts the covariance in one step and updates the covariance. Quantitative descriptions of the quality of the predictions are made using information related to the dynamic characteristics of the system, such as state transfer equations, noise inputs, and process noise variance.

$$\boldsymbol{P}(k+1|k)=\boldsymbol{\Phi}\boldsymbol{P}(k|k)\boldsymbol{\Phi}^{\mathrm{T}}+\boldsymbol{\Gamma}\boldsymbol{Q}\boldsymbol{\Gamma}^{\mathrm{T}}, \tag{7}$$

$$\boldsymbol{P}(k+1)=[\boldsymbol{I}-\boldsymbol{K}\boldsymbol{H}]\boldsymbol{P}+\boldsymbol{P}\boldsymbol{H}^{\mathrm{T}}\boldsymbol{K}^{\mathrm{T}}+\boldsymbol{K}\boldsymbol{H}\boldsymbol{P}\boldsymbol{H}^{\mathrm{T}}\boldsymbol{K}^{\mathrm{T}}+\boldsymbol{K}\boldsymbol{R}\boldsymbol{K}^{\mathrm{T}}, \tag{8}$$

$$\boldsymbol{P}(k+1|k+1)=[\boldsymbol{I}_n-\boldsymbol{K}(\boldsymbol{K}+1)\boldsymbol{H}]\boldsymbol{P}(k+1|k), \tag{9}$$

where $\boldsymbol{K}$, $\boldsymbol{P}$ are abbreviations to the right of the omitted identification; $\boldsymbol{Q}$ is the process noise variance[7]; $\boldsymbol{R}$ is measurement noise variance[7].

2 MP-Huber KF algorithm

2.1 P-Huber weight function based on Mahalanobis distance

How to divide the measured data information into intervals and how to assign weights to each interval[15] are generally summarized as the main part of the equivalent weight function class problem. For example, a typical Huber weight function can be expressed as

$$\bar{w}_k=\begin{cases}1, & |\tilde{v}_b|<c,\\ \dfrac{c}{|\tilde{v}_b|}, & |\tilde{v}_b|\geqslant c,\end{cases} \tag{10}$$

where $|\tilde{v}_b|$ is the absolute value of the normalized residual after calculation, and c is the critical point for discriminating the appearance of outliers. The obtained data is divided into small error interference data and large error interference data.

The Huber weight function is usually not used in real systems because it requires a certain amount of experience, algorithmic knowledge, and data samples to obtain normalized residuals. And the decision threshold needs to be determined based on experience. Therefore, in order to accurately judge the size of outliers and reduce the differentiation tendency of outliers, the probabilistic P-Huber weight function is used to replace the original two-stage function and the Mahalanobis distance function is used to replace the standardized residual of the algorithm. To this end, Mahalanobis distance is introduced to determine the error interference between the measured value at this moment and the estimated value at the previous moment[16,17], then the improved Huber function discriminant is

$$r_k=M_k^2=\left(Y_k-\hat{Y}_{k-1}\right)^{\mathrm{T}}\left(P_{k|k-1}\right)^{-1}\left(Y_k-\hat{Y}_{k-1}\right), \tag{11}$$

$$M_k=\sqrt{\left(Y_k-\hat{Y}_{k-1}\right)^{\mathrm{T}}\left(P_{k|k-1}\right)^{-1}\left(Y_k-\hat{Y}_{k-1}\right)}. \tag{12}$$

Set the measurement noise that satisfies the Gaussian distribution, and the error r_k obeys the chi-square distribution with n_z as the range, so there is

$$p(r_k>x_\alpha)=\alpha, \tag{13}$$

$$\bar{w}_k=\begin{cases}1, & r_k<x_{\alpha_1},\\ \sqrt{\dfrac{x_{\alpha_1}}{r_k}}, & x_{\alpha_1}\leqslant r_k<x_{\alpha_2},\\ 0, & r_k\geqslant x_{\alpha_2},\end{cases} \tag{14}$$

where $p(\cdot)$ is the probability factor in different states, and x_α is set as two chi-square distribution quantiles as x_{α_1} and x_{α_2}. Among them, α_1 and α_2 are two chi-square distributions. When r_k exceeds x_α, the abnormal error interference is determined, and the weight is reassigned. When $r_k\geqslant x_{\alpha_2}$ is satisfied, the large error interference is determined and its distribution capability is eliminated. The method of readjusting the critical value is realized.

2.2 MP-Huber KF algorithm steps

Fig. 2 shows the overall process of Kalman filtering based on Mahalanobis distance weighting function, which is a continuous recursive process of "prediction-correction" in the response time domain.

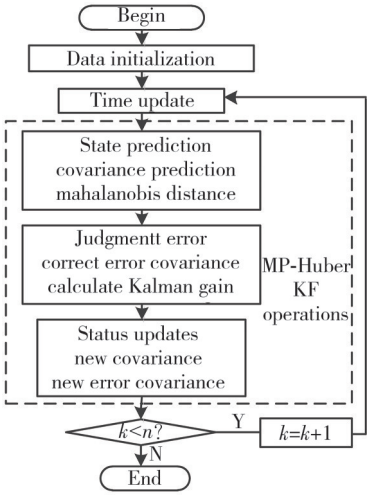

Fig. 2 MP-Huber Kalman filter flow chart

Fig. 3 shows the error interference determination and subsequent process details on the basis of Fig.2.

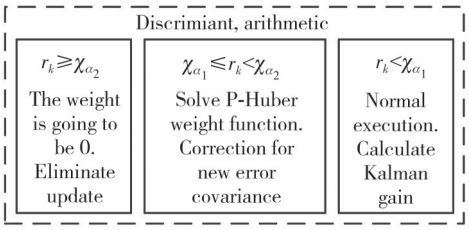

Fig. 3 Detail flow chart

The detailed steps of the MP-Huber Kalman algorithm process are as follows.

Step 1 MP-Huber KF prediction sets $\hat{x}_0 = E[x_0]$ and $P_0 = E\left[(x_0 - \hat{x}_0)(x_0 - \hat{x}_0)^{\mathrm{T}}\right]$ as initial states, and $\boldsymbol{Q}$ and $\boldsymbol{R}$ as covariance matrices. Assume that the temperature measurement value at the $(k-1)$th time (the previous time) is a constant value, the covariance $\boldsymbol{P}(k|k-1)$ is the deviation of the measured value, the thermometer measures the kth time, and the deviation between the measured temperature and the actual temperature is used to estimate the temperature at the time. An estimate that is closest to the true value can be obtained by processing the two sets of data. Realize the temperature value at moment $k-1$ to predict the temperature at the kth time by

$$\hat{\boldsymbol{X}}_{k|k-1} = \boldsymbol{\Phi}\hat{\boldsymbol{X}}_{k-1}, \tag{15}$$

$$P_{k|k-1} = \boldsymbol{\Phi}P_{k-1}\boldsymbol{\Phi} + \boldsymbol{Q}, \tag{16}$$

$$\hat{\boldsymbol{Z}}_{k|k-1} = \boldsymbol{H}\hat{\boldsymbol{X}}_{k|k-1} + \boldsymbol{R}, \tag{17}$$

where $\hat{\boldsymbol{X}}_{k|k-1}$ and $\hat{\boldsymbol{Z}}_{k|k-1}$ are the one-step prediction of the state vector and measurement value at time k; $\boldsymbol{P}_{k|k-1}$ is the prediction covariance; $\boldsymbol{Q}_k$ is the process noise; $\boldsymbol{\Phi}$ and $\boldsymbol{H}$ are the change matrix and state transition matrix on both sides.

Step 2 MP-Huber KF determines whether it is an abnormal error, Eqs. (11) — (14) can be executed through the Mahalanobis distance. When $r_k < x_{\alpha_1}$, the measurement is considered unaffected by outliers, which is a normal error. When $r_k \geqslant x_{\alpha_2}$, it is considered that the measurement has abnormal error due to the influence of outliers. It is considered that outliers seriously affect the measurement accuracy.

Step 3 MP-Huber KF performs different processing according to conditions to generate new states, new filter gains, and new covariances. When it is a normal error, Kalman filtering is performed according to the prior weight, i.e., Eqs. (3) to (9) are performed. If it is judged to be an abnormal error, its weight should be reduced to reduce the influence of outliers. That is, Eqs. (3) and (7) are first performed, and then Eqs. (18) to (23) are performed to obtain the weights by the P-Huber function.

Discriminate errors, and get new state updates, filter gain, and covariance updates.

$$\hat{\boldsymbol{X}}(k+1|k+1) = \hat{\boldsymbol{X}}(k+1|k) + \bar{\boldsymbol{K}}(k+1)\varepsilon(k+1), \tag{18}$$

$$\bar{\boldsymbol{K}}(k+1) = \boldsymbol{P}(k+1|k)\boldsymbol{H}^{\mathrm{T}}\left[\boldsymbol{H}\boldsymbol{P}(k+1|k)\boldsymbol{H}^{\mathrm{T}} + \boldsymbol{R}\right]^{-1}, \tag{19}$$

$$\boldsymbol{P}(k+1|k) = \sum \boldsymbol{w}_j\left(\hat{x}_{k|k} - x_{k|k}\right) \times \left(\hat{x}_{k|k} - x_{k|k}\right)^{\mathrm{T}}, \tag{20}$$

$$\boldsymbol{P}(\bar{K}+1|k+1) = \left[\boldsymbol{I} - \bar{\boldsymbol{K}}(\bar{K}+1)\boldsymbol{H}\right]\boldsymbol{P}(k+1|k). \tag{21}$$

When it is judged to be a large error, reducing its weight to zero can effectively eliminate the influence of large abnormal error on filtering. It is important to note that when $\bar{w}_k = 0$, $P_{k|k-1} \to \infty$, there are

$$\hat{X}_{k|k} = \hat{X}_{k|k-1}, \tag{22}$$

$$P_{k|k} = P_{k|k-1}. \tag{23}$$

3 Multi-information fusion target estimation

Under the premise that each sensor system can independently perform filtering and tracking, each observation station uses the multi-target tracking system to obtain the telemetry data and real-time operating status of local targets through the observed data, and sends them to the fusion center[19]. After a series of measures such as spatial alignment and time calibration, the fusion center will conduct track correlation and select an appropriate fusion method to obtain the state fusion estimate of the required target[20,21].

It can make the data consistent to a great extent by using the improved Kalman filter algorithm. At the same time, more temperature sensors than the original are placed in four important positions, and the fusion value obtained by averaging the four estimated values is input into the temperature control center, so that the car can continue to maintain a suitable temperature. Even if one of the temperature sensors fails, the remaining three can continue to obtain processed fusion values. Therefore, four important positions in the car, such as the front driver and the co-pilot, and the left and right sides of the rear row, are selected as the best places to place the temperature sensors. Fig.4 shows the schematic diagram of the fusion system.

Target tracking information fusion methods[22] are

divided into four categories: estimation theory-based fusion methods, statistical theory-based fusion methods, information theory-based fusion methods and artificial intelligence-based fusion methods.

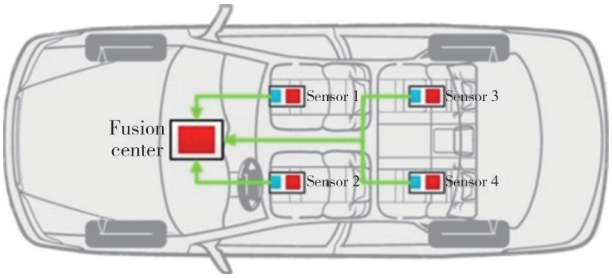

Fig. 4 Diagram of multi-temperature sensor data fusion system in car

Commonly used weighted arithmetic mean fusion methods are discussed. Because each observation station is independent of each other in the measurement process, and the local state estimation error of each observation station is assumed to be independent, so the MP-Huber Kalman filter is used in each observation station.

Step 1 Fusion station estimates each target state through the fused Kalman filter algorithm from the observation information, and records the value of each state as $\hat{x}_k^{(1)}$, $\hat{x}_k^{(2)}$, …, $\hat{x}_k^{(n)}$.

Step 2 The fusion method is used to calculate the weight factor in the fusion process.

$$w_k^{(i)}=\frac{1}{n},(i=1,2,\cdots,n). \tag{24}$$

Step 3 The state estimates of each observatory at each moment are weighted average based on $w_k^{(i)}$ to obtain the fusion estimates corresponding to the target positions.

$$\hat{x}_k=\sum_{i=1}^{n} w_k^{(i)}\hat{x}_k^{(i)}. \tag{25}$$

Step 4 The whole process sets $k=k+1$ and performs the next moment of computational tracking through the continuous operation of steps 1 to 3.

4 Results and discussion

4.1 Normal and abnormal interference

The system model state equations are shown in Eqs. (1) and (2). Assume that the measurement period T is 1 min, the temperature target is observed 500 times, the measurement noise variance is the thermometer variance $R=5\times10^{-2}$, and the temperature state $X(k)$ inside the car is a one-dimensional variable data set that meets the normal distribution at the specified mean and variance. Initially, the measured and real temperature in the car are 25 ℃. The model coefficients are constant $A=1$, $\Gamma=1$. The process noise is $W(k)$, and its variance is Q, which refers to external factors such as the degree of external weather changes, the intensity of sunlight, and the smooth air circulation. Setting the abnormal situation depends on the size of Q. The Kalman estimation error is defined as E_{K}, and MP-Huber Kalman estimation error is defined as E_{MK}.

$$E_{\mathrm{K}}=\left|\hat{\hat{x}}_{k,j}-\hat{x}_{k,j}\right|, \tag{26}$$

$$E_{\mathrm{MK}}=\left|\hat{\bar{x}}_{k,j}-\hat{x}_{k,j}\right|, \tag{27}$$

where $\hat{y}_{k,j}$ is the measured temperature of the jth simulation at time k; $\hat{x}_{k,j}$ is the real temperature of the jth simulation at time k; and $\hat{\hat{x}}_{k,j}$ is the estimation temperature of the jth Kalman filter simulation at time k; $\bar{x}_{k,j}$ is the estimated temperature of the jth improved Kalman filter simulation at time k. Then we take the average value of the two as $\bar{E}_{\mathrm{K}}$ and $\bar{E}_{\mathrm{MK}}$. Finally, different interference error values are set, and the average of 500 groups of estimated errors is calculated. $Q=0.15$ is regarded as normal error interference, $Q=1.5$ is regarded as abnormal error interference, and the Kalman algorithm is compared with MP-Huber Kalman algorithm.

$$\bar{E}_{\mathrm{K}}=\frac{\sum\left|\hat{\hat{x}}_{k,j}-\hat{x}_{k,j}\right|}{500}, \tag{28}$$

$$\bar{E}_{\mathrm{MK}}=\frac{\sum\left|\hat{\bar{x}}_{k,j}-\hat{x}_{k,j}\right|}{500}. \tag{29}$$

Normal error interference is shown as Figs.5 and 6.

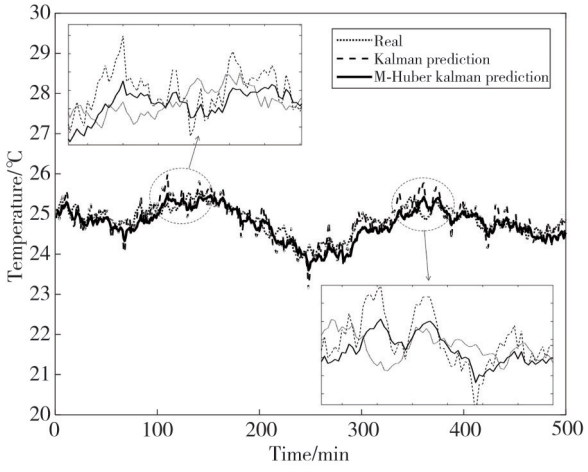

Fig. 5 Performance comparison of normal interference algorithms

As shown in Fig. 5, under normal error interference, both algorithms with observation time of 500 min can track the actual temperature well. Among them, MP-Huber KF gives different reasonable weights according to the interval division, which makes the anti-outlier performance better. The results show that the straight

line is smoother when the requirements of accurate tracking are met.

Fig. 6 shows the error analysis and comparison of the two algorithms under normal conditions. It can be seen intuitively that the maximum value of the discriminant error of the traditional algorithm swings up and down the value of 1, and the average absolute error of the MP-Huber KF algorithm is 0.172, which can be used as an optimal estimation algorithm.

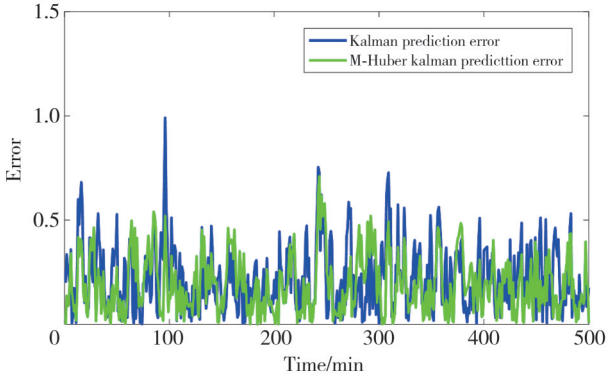

Fig. 6 Error comparison of normal interference algorithms

Abnormal error interference is shown as Figs. 7 and 8. As shown in Fig. 7, in the case of abnormal perturbations, there are significant fluctuations in the observed real data. The fluctuation is 15 ℃ in 200 min. However, the estimates obtained under normal conditions are biased from the simulation results. Therefore, temperature target tracking still belongs to the high precision level. Among them, M Huber Kalman algorithm still maintains the characteristics of good outlier performance, the red real data is closer, and the linear fluctuation is small and smooth.

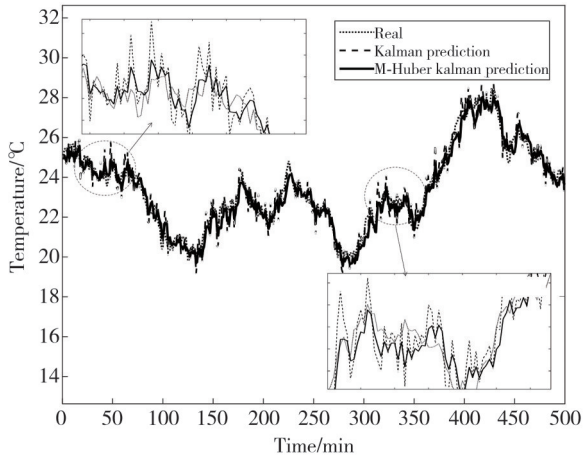

Fig. 7 Performance comparison of abnormal interference algorithms

As shown in Fig. 8, comparing the distance errors of the two algorithms, the maximum absolute error obtained by the Kalman algorithm is below the value of 2, and the average absolute error of the optimized algorithm is 0.342. In the performance detail graph, we can see that the data jitter is greater in the interval of 30 to 80 minutes and 310 to 370 min. It can be seen intuitively that compared with Kalman, the MP-Huber KF algorithm has a great improvement. Under the higher premise, the system robustness is also better.

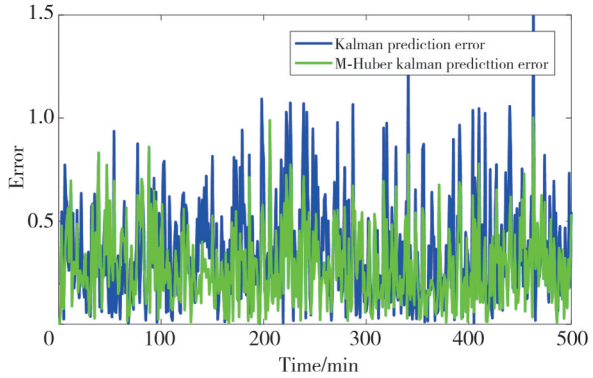

Fig. 8 Error comparison of abnormal interference algorithms

The interference errors are taken as 0.1, 0.3, 0.5, 0.7, 1, and 1.5, respectively. The average estimation errors $\overline{E}_{\mathrm{K}}$ and $\overline{E}_{\mathrm{MK}}$ of the Kalman algorithm and the M-Huber Kalman algorithm are compared in Table 1.

Table 1 Estimation errors of each algorithm

Annoyance value	$\overline{E}_{\mathrm{K}}$	$\overline{E}_{\mathrm{MK}}$
0.1	0.239	0.172
0.3	0.327	0.251
0.5	0.381	0.303
0.7	0.413	0.317
1.0	0.441	0.339
1.5	0.458	0.342

Because the confidence level of Chi-square distribution is used as the judgment threshold, and the Malanobis distance function is used to construct the abnormal error to judge the value, the improved algorithm improves the accuracy of the error judgment, and thus improves the robustness of the system. Based on 500 sampling points, the distinction between small error and large error disturbance is refined. When the error disturbance increases exponentially, the accuracy of both algorithms decreases, and the value of $\overline{E}_{\mathrm{MK}}$ is always below $\overline{E}_{\mathrm{K}}$. When disturbed by 3 times the interference error, the accuracy is 23.2% better than the traditional algorithm. In the case of large error interference (10 times interference), the accuracy is only reduced by 9.3%.

4.2 Multi-information fusion processing

Set the fusion process as a normal error perturbation state, simulate the four-way temperature data that has

completed MP-Huber Kalman filtering, define the vehicle temperature state as $X_1(k)$, $X_2(k)$, $X_3(k)$, $X_4(k)$, and then explore the overall performance of the smoothing process of arithmetic average fusion and weighted arithmetic average fusion to estimate the data, and the whole fusion process lasts 100 min.

The weighted arithmetic mean fusion design enhances the accuracy of the four-way predicted temperature. The system with different information weights is defined by itself. According to the prior knowledge, the predicted value of the front seat temperature is more important. The weight value C_1 of the predicted data filtered by the front seat processor is set as 0.4, and the value C_2 obtained by the rear seat processor is set as 0.1.

Fig. 9 shows the arithmetic mean fusion smoothing simulation result. Fig. 10 shows the weighted arithmetic mean fusion smoothing simulation result.

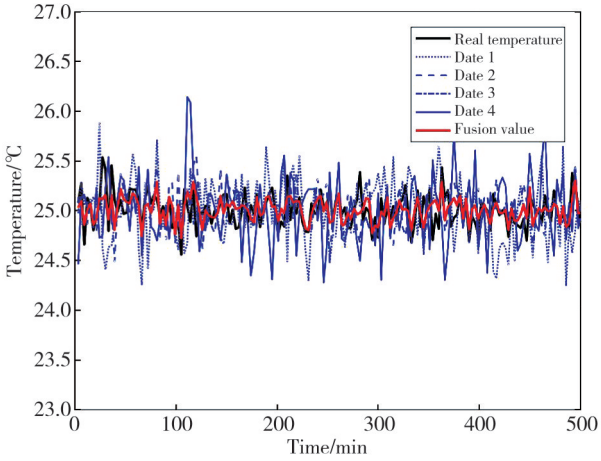

Fig. 9 Simulation of multi-data equal weight fusion processing

The black curve is the final value of the equal-weight fusion process, and its fluctuation is small and smooth compared to the curves of other colors in the Fig. 10. When one of the sensors has a problem, even if the data cannot be collected and uploaded in time, the entire fusion process can still be completed by the other three data processors, and the estimated value obtained by the entire system will not be affected. Due to the local temperature difference in the car body, the most real and accurate data needs to be extracted. Multi-station data fusion can replace the single filter estimation to improve the accuracy of temperature tracking.

As shown in Fig. 10, the fusion value is still smooth. Due to the increased proportion, the black curve is closer to the predicted temperature value of the front seat processor (data 1, data 3). Based on the fusion of 4 groups of data in Fig. 10, in the system for different weighted information processing, the weighted arithmetic average fusion can satisfy the fusion of temperature prediction data in the vehicle with high accuracy.

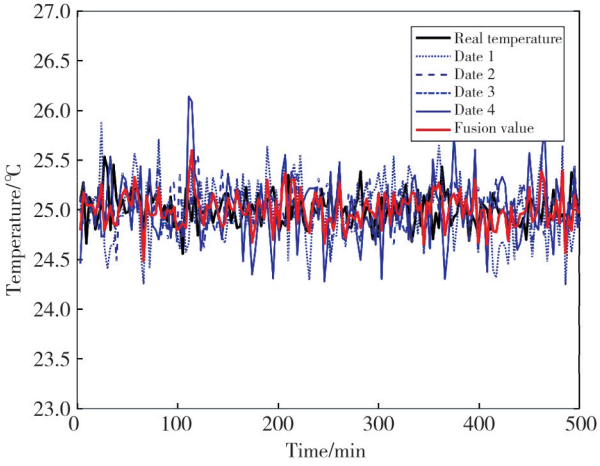

Fig. 10 Weighted arithmetic average fusion processing simulation

The mean value of data 1 of 100 forecast estimates is defined as A_{D1}, and the others are defined as A_{D2}, A_{D3}, and A_{D4}. The mean value of 100 groups of arithmetic average fusion data is defined as A_{F1}, and the mean value of 100 groups of weighted arithmetic average fusion data is defined as A_{F2}. The data pair is shown in Fig. 11.

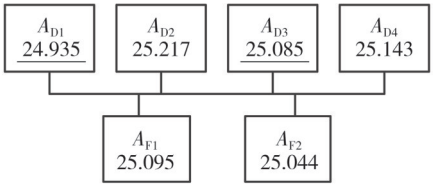

Fig. 11 Data average comparison

The result shows that A_{F2} is closer to A_{D1} and A_{D3}, and its values are similar to those detected by sensors of high importance, achieving the expected results and making the fusion values more accurate.

5 Conclusions

In the process of predicting the temperature state in the vehicle, it is not possible to track the actual temperature accurately when there are abnormal error disturbances. And the single-station processor cannot better estimate the actual temperature of the whole vehicle body. An improved M-Huber Kalman filtering algorithm was proposed based on the classical Kalman filtering. And the sampled data in four places in the vehicle were filtered and then equal-weighted fusion was processed. The system improved the accuracy of the algorithm by improving the method of wild value determination, and also improved the estimation of the overall temperature inside the vehicle by multi-station fusion processing of the data.

1) The improved MP-Huber Kalman algorithm was optimized by constructing the abnormal error determination value by Mahalanobis distance function based on the confidence level of the cardinality distribution. For the appearance of abnormal errors, the wild value interval was accurately judged and given the corresponding weight ration, thus improving the tracking accuracy of the algorithm as well as the stability of the estimated values.

2) The multi-station fusion system could fuse the estimated values of four directions after processing with weighted arithmetic average. The system has better fault tolerance and robustness because it can track the real temperature in the vehicle in a targeted manner and prevent the data variation due to the damage of individual devices.

Acknowledgement

This work was supported by Natural Science Foundation of Gansu Province (No. 20JR5RA407).

Declaration of conflicting interests

The authors have no conflict of interests related to this publication.

References

[1] DUANMU L, SUN X W, JIN Q, et al. Relationship between human thermal comfort and indoor thermal environment parameters in various climatic regions of China. Procedia Engineering, 2017, 205: 2871-2878.

[2] PANG M Y, WANG W B, WANG S Y. Building indoor temperature prediction model based on particle swarm optimization support vector machine. Science and Technology & Innovation, 2017(18): 14-15.

[3] SUN T, JI S X. Modeling and simulation on delay of central heating system for temperature prediction. Journal of System Simulation, 2018, 30(4): 1328-1336.

[4] JWO D J, YANG C F, CHUANG C H, et al. Performance enhancement for ultra-tight GPS/INS integration using a fuzzy adaptive strong tracking unscented Kalman filter. Nonlinear Dynamics, 2013, 73(1): 377-395.

[5] ZHANG Z T, ZHANG J S. Sampling strong tracking nonlinear unscented Kalman filter and its application in eye tracking. Chinese Physics B, 2010, 19(10): 104601.

[6] ZHOU J L, DONG C J. Kalman filtering prediction of loudspeaker coil temperature based on thermal model. Journal of Xi'an Polytechnic University, 2019, 33(6): 631-636.

[7] HANG X P, WANG Y. Kalman filter principle and application: MATLAB simulation. Beijing: Publishing House of Electronics Industry, 2015: 20-24.

[8] YUE Y L, CHEN Y N, SUN Q, et al. Research on multi-sensor data fusion based on biased Kalman. Instrument Technique and Sensor, 2022(1): 82-86.

[9] ZOU H F, LUO T T. An improved Kalman object real-time detection and tracking algorithm. Computer Simulation, 2022, 39(3): 200-204.

[10] LI Q R, SUN F. Strong tracking cubature Kalman filter algorithm for GPS/INS integrated navigation system// 2013 IEEE International Conference on Mechatronics and Automation, August 4-7, 2013, Takamatsu, Japan. New York: IEEE, 2013: 1113-1117.

[11] CHEN S, LU M. Analysis and comparison of several filtering algorithms. Computer Knowledge and Technology, 2020, 16(32): 23-25.

[12] NARAYAN K, MAHESH B, ANDREAS S. An introduction to kalman filtering with MATLAB examples. SenSIP Center, Arizona State University, State of Arizona, 2013: 34-43.

[13] ARMANDO B, MALEK A, FRANCISCO O, et al. Intuitive understanding of Kalman filtering with MATLAB. Florida: Florida International University, 2020: 56-61.

[14] BHAUMIK S, SWATI. Cubature quadrature Kalman filter. IET Signal Processing, 2013, 7(7): 533-541.

[15] JIANG S H, QIAN X M, SHEN J L, et al. Author topic model-based collaborative filtering for personalized POI recommendations. IEEE Transactions on Multimedia, 2015, 17(6): 907-918.

[16] WU H, CHEN S X, YANG B F, et al. Robust cubature Kalman filter target tracking algorithm based on genernalized M-estiamtion. Acta Physica Sinica, 2015, 64(21): 456-463.

[17] REN Z, LI J Y, WU H. Single-observer tracking algorithm based on M-estimation robust backward-smoothing CKF. Computer Engineering and Applications, 2019, 55(11): 74-79.

[18] ARASARATNAM I, HAYKIN S, HURD T R. Cubature Kalman filtering for continuous-discrete systems: theory and simulations. IEEE Transactions on Signal Processing, 2010, 58(10): 4977-4993.

[19] YU Y L. Research on target tracking algorithm based on hybrid filter of UKF and PF. Guilin: Guilin University of Technology, 2019.

[20] GUAN L. Research and implementation of airborne multi-sensor data fusion target tracking technology. Chengdu: University of Electronic Science and Technology of China, 2012.

[21] NONG X Y. Research and implementation of aerial surveillance information fusion technology based on deep learning and Kalman filtering algorithm. Beijing: Beijing University of Posts and Telecommunications, 2021.

[22] HUANG X F. Research and application of multi-sensor target tracking data fusion technology. Beijing: University of Chinese Academy of Sciences, 2012.

基于MP-Huber Kalman滤波的温度预测多信息融合算法

徐万金，李积英*，卢艳东

兰州交通大学 电子与信息工程学院，甘肃 兰州 730070

摘　要：为减少车内温度预测出现野值的错误判断以及提高单站式处理器预测数据精度，本文提出一种基于优化P-Huber权函数的Kalman滤波多信息融合算法。该算法以Kalman滤波作为整体框架，为确立判决阈值需以卡方分布的置信水平作为依据。同时，通过Mahalanobis距离函数构建异常误差判定数值，形成改进后的三段Huber权函数，准确判定野值区间并赋予合理权值配比，从而改善算法跟踪精度。本文还对优化滤波后所得出的车内四路重要地点数据值进行了信息融合处理。理论分析表明，相比于Kalman滤波算法，本文所提算法能在异常误差情形下对实际温度进行准确追踪，且多站式数据融合处理能提高系统整体容错性。结果表明，所提算法能有效降低异常误差对滤波的干扰，且融合处理的综合值更具稳定性和评判性。

关键词：Huber权函数；Mahalanobis距离；Kalman滤波；多信息融合；温度预测

引用格式：XU Wanjin, LI Jiying, LU Yandong. Multi-information fusion algorithm for temperature prediction based on MP-Huber Kalman filter. Journal of Measurement Science and Instrumentation, 2025, 16(2): 236-244. DOI: 10.62756/jmsi.1674-8042.2025023